

# Dalton Transactions

Accepted Manuscript



This is an *Accepted Manuscript*, which has been through the Royal Society of Chemistry peer review process and has been accepted for publication.

*Accepted Manuscripts* are published online shortly after acceptance, before technical editing, formatting and proof reading. Using this free service, authors can make their results available to the community, in citable form, before we publish the edited article. We will replace this *Accepted Manuscript* with the edited and formatted *Advance Article* as soon as it is available.

You can find more information about *Accepted Manuscripts* in the [Information for Authors](#).

Please note that technical editing may introduce minor changes to the text and/or graphics, which may alter content. The journal's standard [Terms & Conditions](#) and the [Ethical guidelines](#) still apply. In no event shall the Royal Society of Chemistry be held responsible for any errors or omissions in this *Accepted Manuscript* or any consequences arising from the use of any information it contains.

1 **Mitochondria-targeted Phosphorescent Iridium(III) Complexes for**  
2 **Living Cell Imaging†**

3 **Qingqing Zhang, ‡<sup>a,b,c</sup> Rui Cao, ‡<sup>a,b</sup> Hao Fei, <sup>a</sup> Ming Zhou\*<sup>a,d</sup>**  
4

5 <sup>a</sup> Division of Nanobiomedicine, Suzhou Institute of Nano-Tech and Nano-Bionics, Chinese Academy of Sciences,  
6 398 Ruoshui Road, Suzhou Industrial Park, Suzhou, Jiangsu, 215125, P. R. China

7 Email: mzhou2007@sinano.ac.cn

8 <sup>b</sup> University of Chinese Academy of Sciences, 19A Yuquan Road, Beijing, 100049, P. R. China

9 <sup>c</sup> Institute of Chemistry, Chinese Academy of Sciences, 2 Zhongguancun North First Street, Beijing 100190, P. R.  
10 China

11 <sup>d</sup> SunaTech Inc., bioBAY, Suzhou Industrial Park, Suzhou, Jiangsu, 215125, P. R. China

12 ‡ Qingqing Zhang and Rui Cao contributed equally to this work.

13 † Electronic Supplementary Information (ESI) available: Ligand synthesis, absorption and emission of  
14 **IrMitoOlivine** and **IrMitoNIR** in PBS, and cell imaging of [Ir(bt)<sub>2</sub>]<sub>2</sub>(bpy-COOH) and [Ir(btphen)<sub>2</sub>]<sub>2</sub>(bpy-COOH).  
15 See DOI: 10.1039/b000000x/  
16

[Insert Running title of <72 characters]

## 1 Abstract

2 Two phosphorescent iridium(III) complexes conjugated to lipophilic triphenylphosphonium cation moiety,  
3 **IrMitoOlivine** and **IrMitoNIR**, were synthesized. The complexes show high mitochondria-specificity and  
4 relatively lower cytotoxicity. Time-lapsed confocal imaging indicates that both complexes exhibit excellent  
5 anti-photobleaching capability under continuous laser irradiation.

## 6 Introduction

7 Mitochondria are primary intracellular bioenergy-producing compartments in eukaryotic cells, which involve  
8 in numerous vital cellular processes, such as oxidative stress<sup>1</sup> and apoptosis<sup>2</sup>. Larger membrane potential of ca.  
9 180 mV (negative inside) across the mitochondrial membrane<sup>3</sup> than other intracellular compartments results in  
10 stronger and selective accumulation and retention of cations<sup>4</sup> inside mitochondria. In contrast to polar cations,  
11 which require protein carriers to pass through the lipid bilayer, lipophilic cations can actively and easily  
12 penetrate the mitochondrial membrane and accumulate inside<sup>3a,4</sup>, such as rosamines<sup>5</sup> and carbocyanines<sup>6</sup>. Other  
13 than both, lipophilic triphenylphosphonium (TPP) cation is nonfluorescent but enables delivery of wide  
14 varieties of bioactive molecules<sup>3b,7</sup>, such as antioxidant<sup>8</sup>, drugs<sup>9</sup>, and biomacromolecules<sup>10</sup>, into mitochondria.  
15 Radioactive isotope labeled TPP cations were reported as positron emission tomography agents in myocardial  
16 and tumor imaging<sup>11</sup>. A lot of organic fluorescent probes linked to TPP cations were applied in mitochondria-  
17 targeted functional cellular imaging, such as zinc ions<sup>12</sup> and hydrogen peroxide<sup>13</sup>.

18 Phosphorescent cyclometalated iridium(III) complexes generally have high quantum efficiencies, large Stokes'  
19 shifts, fine emission tunability and excellent anti-photobleachability<sup>14</sup>, and thus attract extensive interest in  
20 chemosensing<sup>15</sup> and bioimaging<sup>16</sup>. Moreover, phosphorescence properties of iridium(III) complexes depend on  
21 their primary ligands and are able to vary to certain degree with their ancillary ligands. Combining a  
22 phosphorescent iridium(III) complex with a lipophilic TPP cation is a facile way to build up a mitochondria-  
23 specific phosphorescent probe<sup>17</sup> while retaining luminescent properties of the iridium(III) complex herein.  
24 Such a probe was first reported by Murase *et al*<sup>18</sup>. However, the first reported TTP functionalized iridium(III)  
25 complex probe has an acetylacetonato ancillary, which is a labile ligand and can be replaced by coordinating  
26 solvent molecules including water under the attack of protons<sup>19</sup>. Reported in this work are two TTP  
27 functionalized iridium(II) complexes with a stable diimine ancillary ligand (Scheme 1). The change of  
28 acetylacetonato into a 2,2'-bipyridine derivative leads to a change of the electronically neutral state into  
29 electronically positive state of the iridium(III) phosphores. Thus, in addition to avoiding the proton induced  
30 degradation, the positively charged phosphores may have extra advantage over the neutral one, such as better  
31 permeability into cells, and accessibility to molecular modification. Such cationic phosphorescent iridium(III)  
32 complexes have found use in cell imaging<sup>14b,16a,20</sup>.

## 33 Results and discussion

### 34 Design and Synthesis

35 Two biscyclometalated diimine iridium(III) complexes, the yellowish green emitting bis(2-  
36 phenylbenzothiazolato) (4-methyl-4'-carboxypropyl-2,2'-bipyridine) iridium(III) ([Ir(bt)<sub>2</sub>]<sub>2</sub>(bpy-COOH))<sup>21</sup> and  
37 the near infrared (NIR) emitting bis(6-(benzothien-2-yl)phenanthridinato) (4-methyl-4'-carboxypropyl-2,2'-  
38 bipyridyl) iridium(III) ([Ir(btphen)<sub>2</sub>]<sub>2</sub>(bpy-COOH))<sup>22</sup> complexes are chosen as phosphorescent moieties, whose  
39 luminescent emission bands are distinct from those of commercially available MitoTracker<sup>®</sup> Red FM and  
40 Green FM, respectively. The two TPP functionalized probes, **IrMitoOlivine** and **IrMitoNIR** were synthesized  
41 by conjugating carboxy terminals of the corresponding iridium(III) complex and TPP cation with 1,6-  
42 hexamethylene-diamine linker (Scheme 1), and characterized with high-resolution TOF-MS and <sup>1</sup>H/<sup>13</sup>C NMR.  
43 Long linkage was employed to minimize the interplay of the phosphorescent emitter and TPP cation.

[Insert Running title of <72 characters]

## 1 Absorption and Emission Spectroscopy

2 The absorption and emission spectra of **IrMitoOlivine** and **IrMitoNIR** in CH<sub>3</sub>CN are presented in Fig. 1, and  
3 the photophysical data are summarized in Table 1. As designed, **IrMitoOlivine** and **IrMitoNIR** exhibit  
4 yellowish green ( $\lambda_{em}$  527, 563 nm) and NIR ( $\lambda_{em}$  708 nm) phosphorescence with quantum yield  $\Phi_{em} = 0.487$   
5 and 0.032 in N<sub>2</sub>-saturated CH<sub>3</sub>CN. Their <sup>3</sup>MLCT (metal-to-ligand charge transfer) absorption band locates in  
6 the range of 390-500 nm and 450-600 nm, respectively. In aqueous PBS buffer (Fig. S1), the wavelengths of  
7 the absorption bands and emission peaks remained unchanged, but the quantum yields became smaller (0.039  
8 and 0.013 for **IrMitoOlivine** and **IrMitoNIR**, respectively). In comparison with organic dyes, phosphorescent  
9 **IrMitoOlivine** and **IrMitoNIR** display complete separation of the emission bands from their <sup>3</sup>MLCT  
10 absorption regions, which brings advantage in pairing excitation light source and emission detection in a  
11 practical application. Though their emission intensities are sensitive to oxygen concentration ( $\Phi_{em}$  0.035 and  
12 0.012 in air-saturated CH<sub>3</sub>CN, respectively), phosphorescent IrMito dyes are still appropriate in most situations  
13 of biological research.

## 14 Lipophilicity and Cytotoxicity

15 The lipophilicity (logD) of [Ir(bt)<sub>2</sub>]<sub>2</sub>(bpy-COOH), [Ir(btphen)<sub>2</sub>]<sub>2</sub>(bpy-COOH), **IrMitoOlivine** and **IrMitoNIR**  
16 was determined in the n-octanol/PBS (pH 7.4) system. And the cytotoxicity of **IrMitoOlivine** and **IrMitoNIR**  
17 was evaluated using MTT assay in HeLa cells. As expected, compared with [Ir(bt)<sub>2</sub>]<sub>2</sub>(bpy-COOH) and  
18 [Ir(btphen)<sub>2</sub>]<sub>2</sub>(bpy-COOH), which have a hydrophilic carboxy terminus, introduction of the lipophilic TPP  
19 cation increases the lipophilicity and thus the cytotoxicity of delivered molecules<sup>9</sup>. **IrMitoOlivine** and  
20 **IrMitoNIR** showed relatively medium IC<sub>50</sub> (**IrMitoOlivine** 38.7±0.5 μM, **IrMitoNIR** 43.0±0.3 μM) (Figure 2,  
21 Table 2). Therefore, we chose 20 μM of IrMito dyes in the following cell imaging.

## 22 Intracellular localization

23 To demonstrate **IrMitoOlivine** and **IrMitoNIR** specifically localizing in mitochondria, we performed co-  
24 localization imaging experiments using IrMito and MitoTracker<sup>®</sup> dyes to co-label HeLa cells. As given in Fig.  
25 2, the observation showed confocal images of **IrMitoOlivine** (upper FITC channel) and **IrMitoNIR** (lower  
26 Cy5 channel) overlaid nearly completely with that of MitoTracker<sup>®</sup> Red FM (upper Cy5 channel) and Green  
27 FM (lower FITC channel), respectively, indicating both IrMito dyes targeted selectively mitochondria rather  
28 than other intracellular compartments or cytoplasm. In comparison, [Ir(bt)<sub>2</sub>]<sub>2</sub>(bpy-COOH) and  
29 [Ir(btphen)<sub>2</sub>]<sub>2</sub>(bpy-COOH) (20 μM, 5% DMSO) were used to stain the HeLa cells through a similar procedure  
30 for 2 h (Fig. S2). The result revealed, without the TPP moiety, [Ir(bt)<sub>2</sub>]<sub>2</sub>(bpy-COOH) and [Ir(btphen)<sub>2</sub>]<sub>2</sub>(bpy-  
31 COOH) were still able to permeate into the cell but showed well-distributed in the cytoplasm, even though  
32 more concentrated around and little located in the the nucleus.

## 33 Anti-photobleaching

34 The photostability of **IrMitoOlivine** and **IrMitoNIR** compared with organic dyes under continuous laser  
35 irradiation was determined using time-lapsed imaging of IrMito and MitoTracker<sup>®</sup> co-stained HeLa cells.  
36 Time-lapsed imaging proceeded for 100 s with 20 s interval. As shown in Fig. 3, phosphorescent intensity of  
37 IrMito dyes (Fig. 3c FITC and 3d Cy5 channels) remained almost constant (see **IrMitoOlivine.avi** and  
38 **IrMitoNIR.avi** in ESI<sup>†</sup>), while the fluorescence of MitoTracker<sup>®</sup> decreased significantly (MitoTrackerRed.avi  
39 and MitoTrackerGreen.avi in ESI<sup>†</sup>), especially for MitoTracker<sup>®</sup> Red FM. For quantitative analysis, a  
40 photobleaching factor was defined as the following:

$$41 \quad \text{Photobleaching Factor} = \frac{I_t - I_{B,t}}{I_0 - I_{B,0}}$$

[Insert Running title of <72 characters]

1  $I_t$ ,  $I_{B,t}$ ,  $I_0$ ,  $I_{B,0}$  are fluorescence intensity at the time  $t$  and the time of starting the measurements, respectively;  
2 the subscript B denotes background fluorescence intensity. Three cell-inclusive and a background regions were  
3 randomly chosen to quantify their fluorescent intensity with Nikon NIS-Elements AR software. Quantitative  
4 anti-photobleaching analysis indicated statistical emission intensity of **IrMitoOlivine** and **IrMitoNIR**  
5 remained a high stability with a small fluctuation less than 5%; however, fluorescent intensity of the  
6 commercial MitoTracker<sup>®</sup> Red FM and Green FM diminished obviously, up to 50% and 16%, respectively, at  
7 the end of the measurements. The result told mitochondria-targetable phosphorescent dyes were potentially  
8 promising in long-time quantitative imaging in living cells for their excellent anti-photobleaching capability  
9 even under continuous exposure to laser.

## 10 Experimental section

### 11 General Information.

12 1,6-Hexylenediamine, 6-bromocaproic acid and di-tert-butyl dicarbonate ( $\text{Boc}_2\text{O}$ ) were purchased from  
13 Aladdin, triphenylphosphine and n-octanol from Sinopharm, DCC and MTT from Sigma-Aldrich, and HOBT  
14 from GL Biochem. MitoTracker<sup>®</sup> Red FM and MitoTracker<sup>®</sup> Green FM were received from Life  
15 Technologies. 4-(4'-Methyl-2,2'-bipyridin-4-yl)butyric acid (MBBA),  $[\text{Ir}(\text{bt})_2]_2(\mu\text{-Cl})_2$  and  $[\text{Ir}(\text{btphen})_2]_2(\mu\text{-Cl})_2$   
16 were synthesized with the method described in the literatures (ESI<sup>†</sup>). Other chemicals and solvents were  
17 commercially available in analytical grade and used directly except otherwise specified.

18 Human cervical carcinoma HeLa cells were received from Institute of Biochemistry and Cell Biology, SIBS,  
19 CAS. DMEM (Dulbecco's modified Eagle medium), FBS (fetal bovine serum) and penicillin/streptomycin  
20 were purchased from Sigma-Aldrich.

21 GC-MS was determined on Agilent 7890A GC system equipped with 5975C inert triple-axel MS detector.  
22 ESI-TOF-MS was measured on Agilent 1200/6200 TOF-MS system.  $^1\text{H}$  and  $^{13}\text{C}$  NMR spectra were acquired  
23 from Varian 400 MHz NMR spectrometer. Elements analysis (C, N, H) was performed on Vario EL III  
24 Element Analyzer (Elementar). UV-Visible absorption and emission spectra were measured on a Lambda 25  
25 UV/Vis spectrometer (PerkinElmer) and F4600 fluorescence spectrophotometer (Hitachi), respectively.

26 **6-Carboxypentamethylenetriphenylphosphonium bromide (TPPC5H10COOH)**. TPPC5H10COOH was  
27 synthesized in reference to Manning *et al.*<sup>23</sup>. A mixture of triphenylphosphine (7.42 g, 28.3 mmol) and 6-  
28 bromocaproic acid (5.01 g, 25.7 mmol) in xylene (35 ml) was placed in a 100 ml round-bottomed flask  
29 equipped with a water-cooled condenser. The solution was heated to reflux for 4 hours with vigorous stirring  
30 until the solution turned turbid and separated into two phases. When the temperature of solution was down to  
31 40-50 °C, diethyl ether (30 ml) was added slowly with vigorous stirring to give off-white microcrystals, which  
32 were collected by vacuum filtration. The product was washed with diethyl ether twice and then dried *in vacuo*  
33 to afford a white solid (6.28 g, yield 50.5 %). ESI-TOF-MS:  $m/z$  ( $[\text{M}-\text{Br}]^+$ ) calcd 377.1670, found 377.1654.  
34  $^1\text{H}$  NMR (400 MHz,  $\text{CDCl}_3$ )  $\delta$  7.88-7.62 (m, 15H), 3.56 (s, 2H), 2.45-2.27 (m, 2H), 1.64 (s, 6H).  $^{13}\text{C}$  NMR  
35 (101 MHz,  $\text{CDCl}_3$ )  $\delta$  176.0, 135.1, 132.0 (dd,  $J = 297.3, 11.2$  Hz), 117.9 (d,  $J = 86.0$  Hz), 34.0, 29.4 (d,  $J =$   
36 16.1 Hz), 23.9, 22.3 (d,  $J = 51.1$  Hz), 21.9;  $^{31}\text{P}$  NMR (162 MHz,  $\text{CDCl}_3$ )  $\delta$  23.9.

37 **tert-Butyl 6-aminohexylcarbamate (HDABoc)**. HDABoc was synthesized according to Dardonville *et al.*<sup>24</sup>.  
38 To  $\text{CH}_2\text{Cl}_2$  solution of 1,6-hexylenediamine (20.06 g, 172.6 mmol) was added dropwise di-tert-butyl  
39 dicarbonate (7.6 g, 34.8 mmol) dissolved in  $\text{CH}_2\text{Cl}_2$ . After 20 h of stirring at room temperature, the mixture  
40 was filtered. The filtrate was concentrated and re-dissolved in ethyl acetate, washed with water. Removal of  
41 solvent gave a milky liquid (5.36 g, yield 71.2 %). GC-MS:  $m/z$  ( $[\text{M}-\text{Bu}]^+$ ) calcd 159.11, found 159.1.  $^1\text{H}$   
42 NMR (400 MHz,  $\text{CDCl}_3$ ):  $\delta$  4.66 (s, 1H), 3.10 (d,  $J = 6.3$  Hz, 2H), 2.68 (t,  $J = 6.9$  Hz, 2H), 1.44 (s, 9H), 1.52-  
43 1.22 (m, 10H).

[Insert Running title of <72 characters]

1 **[Ir(bt)<sub>2</sub>]<sub>2</sub>(bpy-COOH)** and **[Ir(btphen)<sub>2</sub>]<sub>2</sub>(bpy-COOH)**. [Ir(bt)<sub>2</sub>]<sub>2</sub>(bpy-COOH) and [Ir(btphen)<sub>2</sub>]<sub>2</sub>(bpy-  
2 COOH) were synthesized in a similar way. [Ir(bt)<sub>2</sub>]<sub>2</sub>(bpy-COOH): a mixture of [Ir(bt)<sub>2</sub>]<sub>2</sub>(μ-Cl)<sub>2</sub> (950 mg, 0.77  
3 mmol) and MBBA (421 mg, 1.64 mmol) was refluxed at 80 °C in CH<sub>2</sub>Cl<sub>2</sub>/CH<sub>3</sub>OH mixed solvent until the  
4 solution turned transparent (ca. 2 h). After evaporating off solvents, the product was separated by silica gel  
5 column chromatography (gradient elution with CH<sub>2</sub>Cl<sub>2</sub>/CH<sub>3</sub>OH) to afford orange crystal (1.23 g, yield 89.2%).  
6 ESI-TOF-MS: m/z ([M-Cl]<sup>+</sup>) calcd 869.1596, found 869.1595. <sup>1</sup>H NMR (400 MHz, CDCl<sub>3</sub>) δ 9.32 (s, 1H),  
7 9.01 (s, 1H), 7.90-7.75 (m, 5H), 7.40-7.31 (m, 3H), 7.27 (d, J = 7.4 Hz, 2H), 7.21 (d, J = 5.7 Hz, 1H), 7.14-  
8 7.02 (m, 3H), 6.89-6.81 (m, 2H), 6.38 (dd, J = 7.6, 3.1 Hz, 2H), 6.32-6.27 (m, 1H), 6.25 (d, J = 8.4 Hz, 1H),  
9 2.97 (dt, J = 21.7, 6.9 Hz, 2H), 2.75-2.59 (m, 5H), 2.22 (dd, J = 13.0, 6.6 Hz, 2H); <sup>13</sup>C NMR (101 MHz,  
10 CDCl<sub>3</sub>) δ 181.0, 180.8, 175.0, 156.6, 156.4, 155.9, 152.8, 150.7, 149.9, 149.4, 149.2, 149.1, 140.2, 140.1,  
11 133.4, 133.3, 132.1, 132.0, 131.3, 131.0, 128.8, 128.7, 128.3, 128.2, 126.7, 126.6, 126.5, 126.1, 125.9, 125.8,  
12 123.5, 123.3, 123.1, 123.0, 117.9, 117.7, 34.6, 34.3, 25.5, 21.4. Element analysis (C<sub>41</sub>H<sub>32</sub>N<sub>4</sub>O<sub>2</sub>S<sub>2</sub>ClIr, %): calcd  
13 C 54.44, H 3.57, N 6.09; found C 54.20, H 3.65, N 6.07. [Ir(btphen)<sub>2</sub>]<sub>2</sub>(bpy-COOH): [Ir(btphen)<sub>2</sub>]<sub>2</sub>(μ-Cl)<sub>2</sub>  
14 (867 mg, 0.51 mmol) and MBBA (264 mg, 1.03 mmol) were dissolved in CH<sub>2</sub>Cl<sub>2</sub>/CH<sub>3</sub>OH solution, and  
15 refluxed to turn transparent. After filtration and removal of solvents, the residue was separated similar to  
16 [Ir(bt)<sub>2</sub>]<sub>2</sub>(bpy-COOH) to afford dark red crystal (925mg, yield 82.1%). ESI-TOF-MS: m/z ([M-Cl]<sup>+</sup>) calcd  
17 1069.2222, found 1069.2227. <sup>1</sup>H NMR (400 MHz, cdcl3) δ 9.39 (s, 2H), 8.61 (s, 2H), 8.46 (s, 1H), 8.28 (s,  
18 5H), 8.03-7.81 (m, 6H), 7.18 (dt, J = 44.0, 12.8 Hz, 10H), 6.71 (dd, J = 23.8, 14.8 Hz, 6H), 2.65 (s, 2H), 2.39  
19 (s, 5H), 1.87 (s, 2H); <sup>13</sup>C NMR (101 MHz, CDCl<sub>3</sub>) δ 175.2, 167.9, 167.8, 159.5, 159.2, 156.3, 155.1, 155.0,  
20 152.8, 145.6, 145.5, 143.7, 143.6, 143.5, 138.6, 138.4, 133.7, 133.6, 133.3, 128.9, 128.7, 128.4, 128.1, 127.9,  
21 127.8, 127.7, 127.3, 127.0, 126.9, 126.7, 125.6, 125.4, 124.8, 124.7, 124.1, 124.0, 122.9, 122.8, 122.8, 122.7,  
22 122.7, 122.6, 122.1, 122.0, 34.1, 34.0, 25.5, 21.1. Element analysis (C<sub>57</sub>H<sub>40</sub>N<sub>4</sub>O<sub>2</sub>S<sub>2</sub>ClIr, %): calcd C 61.97, H  
23 3.65, N 5.07; found C 61.76, H 3.70, N 5.05.

24 **[Ir(bt)<sub>2</sub>]<sub>2</sub>(bpy-Boc)** and **[Ir(btphen)<sub>2</sub>]<sub>2</sub>(bpy-Boc)**. [Ir(bt)<sub>2</sub>]<sub>2</sub>(bpy-Boc) and [Ir(btphen)<sub>2</sub>]<sub>2</sub>(bpy-Boc) were  
25 synthesized similarly. [Ir(bt)<sub>2</sub>]<sub>2</sub>(bpy-Boc): a mixture of [Ir(bt)<sub>2</sub>]<sub>2</sub>(bpy-COOH) (361 mg, 0.40 mmol), HDABoc  
26 (130 mg, 0.60 mmol), DCC (203 mg, 0.98 mmol) and HOBT (65 mg, 0.48 mmol) was stirred in 10 ml of  
27 anhydrous DMF at room temperature under N<sub>2</sub> protection overnight. After freezing, filtration and removal of  
28 the solvent, the residual solid was separated prudently by silica gel column chromatography  
29 (CH<sub>2</sub>Cl<sub>2</sub>/C<sub>2</sub>H<sub>5</sub>OH=20:1) to afford yellow powder (382 mg, yield 86.6%). ESI-TOF-MS: m/z ([M-Cl]<sup>+</sup>) calcd  
30 1067.3328, found 1067.3298. <sup>1</sup>H NMR (400 MHz, CDCl<sub>3</sub>) δ 8.52 (d, J = 7.2 Hz, 2H), 7.87 (ddd, J = 10.1, 9.6,  
31 5.6 Hz, 4H), 7.79 (ddd, J = 7.7, 4.4, 0.8 Hz, 2H), 7.39-7.30 (m, 3H), 7.28-7.23 (m, 1H), 7.14 (td, J = 8.4, 1.0  
32 Hz, 2H), 7.09-7.03 (m, 2H), 6.85 (dd, J = 10.8, 4.2 Hz, 2H), 6.37 (d, J = 7.7 Hz, 2H), 6.20 (d, J = 8.4 Hz, 1H),  
33 6.13 (d, J = 8.4 Hz, 1H), 3.11 (dd, J = 12.7, 6.7 Hz, 2H), 3.04 (t, J = 6.8 Hz, 2H), 2.89 (t, J = 7.7 Hz, 2H), 2.62  
34 (s, 3H), 2.38 (t, J = 7.5 Hz, 2H), 2.12-2.01 (m, 2H), 1.43 (s, 13H), 1.23 (s, 4H). [Ir(btphen)<sub>2</sub>]<sub>2</sub>(bpy-Boc): the  
35 mixture of [Ir(btphen)<sub>2</sub>]<sub>2</sub>(bpy-COOH) (113 mg, 0.102 mmol), HDABoc (49.8 mg, 0.230 mmol), DCC (71.4  
36 mg, 0.346 mmol) and HOBT (15.4 mg, 0.116 mmol) was dissolved in super-dry DMF (5 ml) and reacted at 0  
37 °C for 24 h. The purification procedure was similar to [Ir(bt)<sub>2</sub>]<sub>2</sub>(bpy-Boc). Dark red powder (112 mg, yield  
38 84.3%). ESI-TOF-MS: m/z ([M-Cl]<sup>+</sup>) calcd 1267.3954, found 1267.3967. <sup>1</sup>H NMR (400 MHz, CDCl<sub>3</sub>) δ 9.44-  
39 9.35 (m, 2H), 8.78 (s, 1H), 8.64-8.56 (m, 2H), 8.27 (dd, J = 11.6, 5.7 Hz, 4H), 8.04-7.91 (m, 5H), 7.87 (d, J =  
40 7.7 Hz, 2H), 7.71 (dd, J = 24.8, 8.4 Hz, 1H), 7.35-7.12 (m, 5H), 7.07 (dd, J = 22.3, 5.7 Hz, 2H), 6.81-6.60 (m,  
41 6H), 3.00 (d, J = 6.2 Hz, 2H), 2.64 (s, 2H), 2.39 (d, J = 4.3 Hz, 3H), 2.23 (d, J = 7.1 Hz, 2H), 1.89 (s, 2H),  
42 1.55-1.06 (m, 19H).

43 **IrMitoOlivine** and **IrMitoNIR**. **IrMitoOlivine** and **IrMitoNIR** were synthesized with a similar method.  
44 **IrMitoOlivine**: after de-protection of [Ir(bt)<sub>2</sub>]<sub>2</sub>(bpy-Boc) (253 mg, 0.229 mmol), the residue was stirred with  
45 TPPC5H10COOH (158 mg, 0.346 mmol), DCC (119 mg, 0.577 mmol) and HOBT (38.2 mg, 0.282 mmol) in  
46 anhydrous DMF (7.5 ml) at room temperature for 24 h. Then 30 ml of saturated NH<sub>4</sub>PF<sub>6</sub> aqueous solution was  
47 added to precipitate the product. The filter-out was then separated by silica gel column chromatography  
48 (gradient elution with CH<sub>2</sub>Cl<sub>2</sub>/CH<sub>3</sub>OH). Yellow crystal, 268 mg, yield 72.4%. ESI-TOF-MS: m/z ([M-2PF<sub>6</sub>]<sup>2+</sup>)  
49 calcd 663.2185, found 663.2157. <sup>1</sup>H NMR (400 MHz, CDCl<sub>3</sub>) δ 8.47 (d, J = 3.9 Hz, 1H), 8.42 (d, J = 2.0 Hz,  
50 1H), 7.91 (dt, J = 14.1, 7.5 Hz, 4H), 7.83-7.73 (m, 5H), 7.73-7.61 (m, 15H), 7.57-7.52 (m, 1H), 7.50-7.43 (m,  
[Insert Running title of <72 characters]

1 1H), 7.38-7.28 (m, 4H), 7.18-7.09 (m, 2H), 7.08-6.99 (m, 2H), 6.87-6.78 (m, 2H), 6.38 (dd, J = 9.8, 2.3 Hz,  
 2 2H), 6.26-6.18 (m, 1H), 6.12 (dd, J = 15.0, 8.4 Hz, 1H), 3.29 (dd, J = 14.0, 7.1 Hz, 2H), 3.08 (ddd, J = 22.8,  
 3 19.7, 9.9 Hz, 6H), 2.91 (d, J = 34.4 Hz, 2H), 2.58 (d, J = 3.1 Hz, 3H), 2.39 (t, J = 7.4 Hz, 1H), 2.28 (t, J = 7.2  
 4 Hz, 3H), 2.13 (dd, J = 14.3, 7.3 Hz, 2H), 2.01 (dd, J = 13.8, 6.7 Hz, 2H), 1.64 (s, 10H); <sup>13</sup>C NMR (101 MHz,  
 5 CDCl<sub>3</sub>) δ 181.1, 177.3, 174.6, 173.9, 173.6, 173.2, 156.6, 156.4, 156.2, 156.1, 156.0, 155.9, 152.7, 150.4,  
 6 150.2, 149.8, 149.1, 149.0, 140.1, 139.0, 135.2, 133.3, 133.2, 132.0, 131.9, 131.8, 131.3, 130.6, 130.5, 128.8,  
 7 128.7, 128.5, 128.2, 127.4, 126.7, 126.6, 126.0, 123.6, 123.1, 118.2, 117.3, 116.2, 111.6, 77.6, 77.5, 77.3, 77.0,  
 8 53.7, 42.5, 40.6, 39.5, 38.6, 35.7, 33.4, 33.0, 32.3, 29.5, 29.3, 28.6, 26.6, 26.0, 25.2, 24.7, 24.5, 23.8, 22.1, 22.0  
 9 21.6, 21.2, 14.1, 12.8; <sup>31</sup>P NMR (162 MHz, CDCl<sub>3</sub>) δ 23.2. Element analysis (C<sub>71</sub>H<sub>70</sub>F<sub>12</sub>N<sub>6</sub>O<sub>2</sub>P<sub>3</sub>S<sub>2</sub>Ir, %): calcd  
 10 C 52.75, H 4.36, N 5.20; found C 52.63, H 4.42, N 5.08. **IrMitoNIR**: a mixture of de-protected  
 11 [Ir(btphen)<sub>2</sub>]<sub>2</sub>(bpy-Boc) (65.2 mg, 54.2 μmol), TPPC5H10COOH (37.8 mg, 82.9 μmol), DCC (25 mg, 121  
 12 μmol) and HOBt (9.25 mg, 68.5 μmol) was stirred in super-dry DMF (3 ml) under inert gas protection at 0 °C  
 13 for 24 h. After precipitation in saturated NH<sub>4</sub>PF<sub>6</sub> solution (30 ml), the solid was then separated by silica gel  
 14 column chromatography (gradient elution with CH<sub>2</sub>Cl<sub>2</sub>/CH<sub>3</sub>OH) to afford red crystal (61.2 mg, yield 62.1%).  
 15 ESI-TOF-MS: m/z ([M-2PF<sub>6</sub>]<sup>2+</sup>) calcd 763.2498, found 763.2516. <sup>1</sup>H NMR (400 MHz, CDCl<sub>3</sub>) δ 9.43-9.36 (m,  
 16 2H), 8.66-8.56 (m, 2H), 8.41-8.26 (m, 4H), 8.03-7.94 (m, 4H), 7.92 (s, 1H), 7.89-7.83 (m, 3H), 7.78 (dd, J =  
 17 10.2, 4.5 Hz, 3H), 7.73-7.59 (m, 13H), 7.32-7.27 (m, 2H), 7.15 (dddd, J = 14.5, 11.2, 9.5, 4.1 Hz, 5H), 6.72  
 18 (dd, J = 13.6, 7.8 Hz, 4H), 6.65 (dd, J = 11.3, 4.0 Hz, 2H), 3.31-2.99 (m, 8H), 2.66-2.54 (m, 2H), 2.33 (s, 5H),  
 19 2.23 (s, 4H), 1.76 (d, J = 27.9 Hz, 2H), 1.72-1.53 (m, 10H); <sup>13</sup>C NMR (101 MHz, CDCl<sub>3</sub>) δ 177.7, 176.9,  
 20 173.7, 173.0, 172.1, 167.9, 165.8, 163.1, 159.2, 159.1, 154.9, 154.8, 152.7, 146.3, 145.6, 143.6, 139.5, 138.6,  
 21 138.5, 135.2, 133.3, 133.2, 131.9, 131.8, 130.6, 130.5, 128.8, 128.6, 128.4, 127.9, 127.0, 126.7, 125.4, 124.9,  
 22 124.7, 124.0, 122.8, 122.6, 122.1, 118.2, 117.3, 116.6, 111.4, 53.6, 42.5, 40.6, 38.6, 34.9, 33.5, 32.3, 29.7,  
 23 29.6, 29.5, 29.4, 29.3, 26.0, 24.5, 24.3, 23.8, 22.2, 22.1, 22.0, 21.8, 21.7, 21.6, 14.1, 12.9, 53.6, 42.5, 40.6,  
 24 38.6, 34.9, 33.5, 32.3, 29.7, 29.6, 29.5, 29.4, 29.3, 26.0, 24.5, 24.3, 23.8, 22.2, 22.1, 22.0, 21.8, 21.7, 21.6,  
 25 14.1, 12.9; <sup>31</sup>P NMR (162 MHz, CDCl<sub>3</sub>) δ 23.3. Element analysis (C<sub>87</sub>H<sub>78</sub>F<sub>12</sub>N<sub>6</sub>O<sub>2</sub>P<sub>3</sub>S<sub>2</sub>Ir, %): calcd C 57.51, H  
 26 4.33, N 4.63; found C 57.34, H 4.18, N 4.58.

## 27 Absorption and Emission Spectroscopy

28 The absorption and emission spectra were recorded in CH<sub>3</sub>CN (UPLC grade, Acros) and DMSO/PBS (2  
 29 vol.%) at room temperature. Quantum yields of **IrMitoOlivine** and **IrMitoNIR** were determined in N<sub>2</sub>- and  
 30 air-saturated CH<sub>3</sub>CN and DMSO/PBS (2 vol.%) with Ru(bpy)<sub>3</sub><sup>2+</sup> in aerated CH<sub>3</sub>CN as a reference  
 31 (Φ=0.062<sup>25</sup>), and calculated with the following equation:

$$32 \quad \Phi_{\text{sam}} = \Phi_{\text{ref}} \times \frac{I_{\text{sam}}}{I_{\text{ref}}} \times \frac{A_{\text{ref}}}{A_{\text{sam}}} \times \frac{n_{\text{sam}}^2}{n_{\text{ref}}^2}$$

33 where, Φ, I, A, n are quantum yield, integral emission intensity, absorbance and refractive index of the  
 34 solvents in which the sample or reference dissolved, respectively.

## 35 Lipophilicity

36 The lipophilicity of **IrMitoOlivine** and **IrMitoNIR** was determined in the n-octanol/PBS (pH 7.4) system  
 37 using the conventional flask-shaking method, which was expressed as logD for ionized compounds. PBS and  
 38 n-octanol were mixed vigorously for 24 h and then the mixture stood still for another 24 h to saturate each  
 39 other. The excessive analyte was dissolved in n-octanol (saturated with PBS) phase for 24 h to obtain a  
 40 saturated solution, whose concentration was donated as C<sub>o</sub>. The saturated n-octanol solution was mixed then  
 41 with equal volume of PBS (saturated with n-octanol) and shaken in an oscillator for 24 h. After partition, the  
 42 concentration in n-octanol phase was donated as C<sub>o</sub>'. The lipophilicity logD was calculated with the following  
 43 equation: logD=log[C<sub>o</sub>'/(C<sub>o</sub>-C<sub>o</sub>')]. The concentration was measured with fluorescent spectrophotometry

[Insert Running title of <72 characters]

1 (**IrMitoOlivine**: ex 411 nm, em 526; **IrMitoNIR**, ex 504 nm, em 708 nm ). The data were determined in  
2 triplicate parallelly and expressed as mean  $\pm$  standard deviation.

### 3 **MTT Assay**

4 MTT assay of **IrMitoOlivine** and **IrMitoNIR** in HeLa cells was carried out to detect their cytotoxicity. HeLa  
5 cells (ca.  $1 \times 10^4$  cells/well) in the exponential phase were seed into 96-well plate (Corning) and incubated in  
6 DMEM supplemented with 10% FBS containing 1% penicillin/streptomycin for 24 h before treatment.  
7 **IrMitoOlivine** or **IrMitoNIR** in DMSO (100-3.13  $\mu$ M) were mixed into 1 mL fresh DMEM/FBS and added  
8 into each well and incubated for another 24 h at 37°C under 5% CO<sub>2</sub> environment. Furthermore, MTT (3-(4,5-  
9 dimethylthiazol-2-yl)-2,5-diphenyltetrazolium bromide) in PBS buffer (5 mg/ml) was added and the cells grew  
10 for more 4 h. After removal of MTT solution, 150  $\mu$ l of DMSO was added to each well and incubated in 37 °C  
11 for 15 min. The OD490 value of each sample was measured with a Victor X4 microplate reader (Perkin-  
12 Elmer). The assay was performed three times independently and in triplicate parallelly each time. IC<sub>50</sub> values  
13 were calculated in SPSS 18 and presented as mean  $\pm$  standard deviation.

### 14 **Cell Staining**

15 HeLa cells were plated on 35 mm cell culture dish (Corning) at density of  $1-2 \times 10^4$  cells/dish. After incubation  
16 for 24 at 37°C under 5% CO<sub>2</sub>, cells were co-stained with **IrMitoOlivine** (20  $\mu$ M)/MitoTracker<sup>®</sup> Red FM (200  
17 nM) or **IrMitoNIR** (20  $\mu$ M)/MitoTracker<sup>®</sup> Green RM (100 nM) in 1 ml DMEM/FBS medium for 30 min,  
18 respectively. After replacement with fresh medium, the cells was imaged with a Nikon A1R confocal laser  
19 scanning microscope for intracellular localization of IrMito dyes. Moreover, for *in vivo* anti-photobleaching  
20 assay of IrMito dyes, time-lapsed cell images were collected continuously with 20 s intervals for 100 s.  
21 Fluorescence intensities of three stochastically chosen cell-inclusive regions were acquired with NIS-Elements  
22 AR software (Nikon), and calculated their photobleaching factors. The data were presented as mean  $\pm$  standard  
23 deviation.

### 24 **Conclusion**

25 In conclusion, two phosphorescent iridium(III) complexes conjugated with the lipophilic  
26 triphenylphosphonium cation, **IrMitoOlivine** and **IrMitoNIR**, were rationally designed and synthesized. Both  
27 complexes demonstrated their specificity to mitochondria. Quantitative photobleaching analysis revealed their  
28 excellent anti-photobleaching capability in continuous living cell imaging. In particular, we demonstrated a  
29 facile method of combining intracellular compartmental specificity with chemically stable phosphorescent  
30 iridium(III) complex reporter, making such phosphorescent metal complexes promising for building up more  
31 organelle-targeted probes.

### 32 **Acknowledgements**

33 This work was financially supported by Natural Science Foundation of China (Grant Nos. 21005084,  
34 21072218). We thank Wanfei Li for his suggestive direction in the synthesis of ligands.

### 35 **Legends**

36 **Scheme 1** Synthesis of **IrMitoOlivine** and **IrMitoNIR**. i) MBBA, CH<sub>2</sub>Cl<sub>2</sub>/CH<sub>3</sub>OH (50 vol.%), 80 °C, 2-4 h;  
37 ii) HDABoc; DCC/HOBt/DMF, r.t., 24 h; iii) TFA/CH<sub>2</sub>Cl<sub>2</sub> (20 vol.%), r.t, 2 h; iv) TPPC5H10COOH,  
38 DCC/HOBt/DMF, r.t., 24 h; NH<sub>4</sub>PF<sub>6</sub>..

39 **Fig. 1** Absorption (dash dot) and emission (solid: N<sub>2</sub>-saturated; dot: air-saturated) spectra of **IrMitoOlivine**  
40 and **IrMitoNIR** in CH<sub>3</sub>CN. The right top inset gives normalized emission spectra. Ex: **IrMitoOlivine**, 411

[Insert Running title of <72 characters]

1 nm; **IrMitoNIR**, 504 nm. The photograph insets show the appearance of **IrMitoOlivine** and **IrMitoNIR** under  
2 natural (left top) and under UV (right bottom) light, respectively.

3 **Fig. 2** Cytotoxicity ( $IC_{50}$ ) of **IrMitoOlivine** and **IrMitoNIR** in HeLa cells.

4 **Fig. 3** Cell imaging of **IrMitoOlivine** and **IrMitoNIR** showed co-localization of MitoTracker<sup>®</sup> and IrMito  
5 dyes in HeLa Cells. Channel: FITC, Ex 488 nm, Em 500-530 nm; Cy5, Ex 561 nm, Em 662-737 nm. Scalar  
6 bar: 20  $\mu$ m.

7 **Fig. 4** Anti-photobleaching observation of **IrMitoOlivine** and **IrMitoNIR** in HeLa cells. (a) (b) Quantitative  
8 photobleaching results showed **IrMitoOlivine** and **IrMitoNIR** possessed robust emission intensity under  
9 continuous light irradiation. The data were represented as mean  $\pm$  standard deviation. (c) (d) Time-lapsed  
10 confocal imaging of **IrMitoOlivine**/MitoTracker<sup>®</sup> Red FM or **IrMitoNIR**/MitoTracker<sup>®</sup> Green FM co-stained  
11 HeLa cells. Blue and red ROIs represented three stochastically chosen cell-inclusive regions and the  
12 background region, respectively. Time interval: 20 s. Scalar bar: 20  $\mu$ m.

### 13 Tables

14

Table 1 Photophysical data of **IrMitoOlivine** and **IrMitoNIR**

Compound	$\lambda_{\text{abs}}/\text{nm}$ ( $\epsilon/10^3 \text{ M}^{-1} \cdot \text{cm}^{-1}$ )	$\lambda_{\text{em}}/\text{nm}$	$\Phi_{\text{em}}^{\text{b}}$
<b>IrMitoOlivine</b>	CH <sub>3</sub> CN <sup>a</sup> 309 (33.8), 322 (31.4), 381 (7.10, sh), 411 (6.88)	527, 563	0.487 <sup>c</sup> 0.035 <sup>d</sup>
	PBS <sup>e</sup> 311 (32.3), 324 (29.7), 381 (7.86, sh), 414 (7.16)	526, 563	0.039
<b>IrMitoNIR</b>	CH <sub>3</sub> CN <sup>a</sup> 334 (23.7), 370 (19.5), 394 (17.5, sh), 503 (5.83)	708	0.032 <sup>c</sup> 0.012 <sup>d</sup>
	PBS <sup>e</sup> 336 (23.0), 373 (18.8), 396 (16.6, sh), 509 (9.02)	706	0.013

15 <sup>a</sup> Absorption and emission spectra were recorded in CH<sub>3</sub>CN; <sup>b</sup> Quantum yields ( $\Phi_{\text{em}}$ ) were determined using  
16 Ru(bpy)<sub>3</sub><sup>2+</sup> ( $\Phi_{\text{em}}=0.062$ ) as reference. <sup>c</sup> In N<sub>2</sub>-saturated CH<sub>3</sub>CN; <sup>d</sup> in air-saturated CH<sub>3</sub>CN. <sup>e</sup> Absorption and  
17 emission spectra were recorded in DMSO/PBS (2 vol.%).

18

Table 2. Cytotoxicity and lipophilicity of **IrMitoOlivine** and **IrMitoNIR**

Compound	$IC_{50}/\mu\text{M}$	$\text{LogD}^{\text{a}}$
[Ir(bt) <sub>2</sub> ] <sub>2</sub> (bpy-COOH)	53.6 $\pm$ 0.6	1.03 $\pm$ 0.03
<b>IrMitoOlivine</b>	38.7 $\pm$ 0.5	1.38 $\pm$ 0.05
[Ir(btphen) <sub>2</sub> ] <sub>2</sub> (bpy-COOH)	48.3 $\pm$ 0.5	1.27 $\pm$ 0.05
<b>IrMitoNIR</b>	43.0 $\pm$ 0.3	1.52 $\pm$ 0.04

19 <sup>a</sup>  $\text{logD}=\text{log}[C_o'/(C_o-C_o')]$ , where  $C_o$  and  $C_o'$  represented molar concentration of the analyte in n-octanol phase  
20 (saturated with PBS) before and after partition.

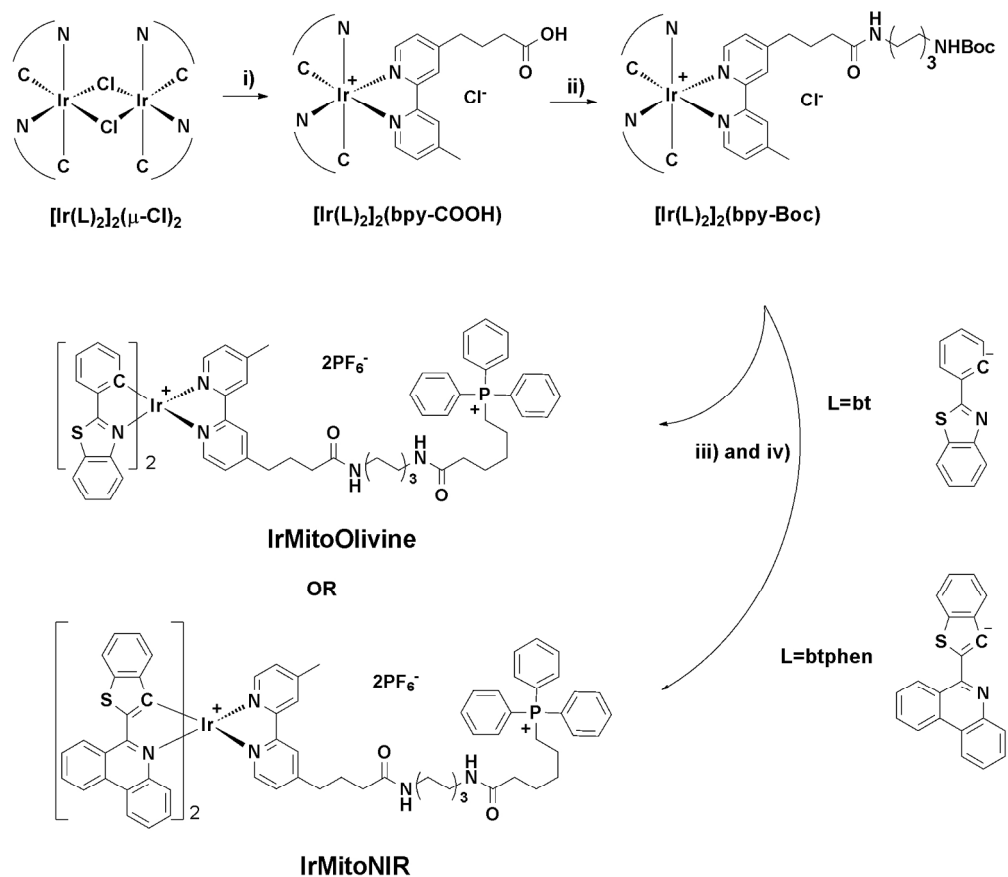
### 21 Notes and references

[Insert Running title of <72 characters]

- 1 (a) G. C. Kujoth, A. Hiona, T. D. Pugh, S. Someya, K. Panzer, S. E. Wohlgemuth, T. Hofer, A. Y. Seo, R. Sullivan, W. A. Jobling, J. D. Morrow, H. Van Remmen, J. M. Sedivy, T. Yamasoba, M. Tanokura, R. Weindruch, C. Leeuwenburgh and T. A. Prolla, *Science*, 2005, 309, 481-484; (b) M. T. Lin and M. F. Beal, *Nature*, 2006, 443, 787-795; (c) E. Cadenas and K. J. A. Davies, *Free Radical Bio. Med.*, 2000, 29, 222-230.
- 2 (a) D. R. Green and J. C. Reed, *Science*, 1998, 281, 1309-1312; (b) G. Kroemer, B. Dallaporta and M. Resche-Rigon, *Annu. Rev. Physiol.*, 1998, 60, 619-642; (c) X. Wang, *Genes Dev.*, 2001, 15, 2922-2933.
- 3 (a) L. B. Chen, *Ann. Rev. Cell Biol.*, 1988, 4, 155-181; (b) M. P. Murphy, *Trends Biotechnol.*, 1997, 15, 326-330.
- 4 S. Davis, M. J. Weiss, J. R. Wong, T. J. Lampidis and L. B. Chen, *J. Biol. Chem.*, 1985, 260, 13844-13850.
- 5 For example, Rhodamine 123, L. V. Johnson, M. L. Walsh and L. B. Chen, *Proc. Natl. Acad. Sci. USA*, 1980, 77, 990-994. MitoTracker<sup>®</sup> Orange CMTMRos and Red CMXRos available from Life Technologies also belong to this class.
- 6 For example, JC-1, M. Reers, T. W. Smith and L. B. Chen, *Biochemistry*, 1991, 30, 4480-4486. MitoTracker<sup>®</sup> Green FM, Red FM and Deep Red FM available from Life technologies also belong to this class.
- 7 R. A. J. Smith, C. M. Porteous, A. M. Gane and M. P. Murphy, *Proc. Natl. Acad. Sci. USA*, 2003, 100, 5407-5412.
- 8 M. P. Murphy and R. A. J. Smith, *Annu. Rev. Pharmacol. Toxicol.*, 2007, 47, 629-656.
- 9 M. P. Murphy and R. A. J. Smith, *Adv. Drug Deliver. Rev.*, 2000, 41, 235-250.
- 10 A. Muratovska, R. N. Lightowers, R. W. Taylor, J. A. Wilce and M. P. Murphy, *Adv. Drug Deliver. Rev.*, 2001, 49, 189-198.
- 11 (a) D.-Y. Kim, H.-J. Kim, K.-H. Yu and J.-J. Min, *Bioconjugate Chem.*, 2012, 23, 431-437; (b) Y. Zhou and S. Liu, *Bioconjugate Chem.*, 2011, 22, 1459-1472.
- 12 (a) K. Sreenath, J. R. Allen, M. W. Davidson and L. Zhu, *Chem. Commun.*, 2011, 47, 11730-11732; (b) G. Masanta, C. S. Lim, H. J. Kim, J. H. Han, H. M. Kim and B. R. Cho, *J. Am. Chem. Soc.*, 2011, 133, 5698-5700; (c) N. Y. Baek, C. H. Heo, C. S. Lim, G. Masanta, B. R. Cho and H. M. Kim, *Chem. Commun.*, 2012, 48, 4546-4548.
- 13 (a) B. C. Dickinson and C. J. Chang, *J. Am. Chem. Soc.*, 2008, 130, 9638-9639; (b) B. C. Dickinson, D. Srikanth and C. J. Chang, *Curr. Opin. Chem. Biol.*, 2010, 14, 50-56; (c) G. Masanta, C. H. Heo, C. S. Lim, S. K. Bae, B. R. Cho and H. M. Kim, *Chem. Commun.*, 2012, 48, 3518-3520.
- 14 (a) C. Adachi, M. A. Baldo, M. E. Thompson and S. R. Forrest, *J. Appl. Phys.*, 2001, 90, 5048-5051; (b) M. Yu, Q. Zhao, L. Shi, F. Li, Z. Zhou, H. Yang, T. Yi and C. Huang, *Chem. Commun.*, 2008, 2115-2117; (c) Y. Chen, L. Qiao, B. Yu, G. Li, C. Liu, L. Ji and H. Chao, *Chem. Commun.*, 2013, 49, 11095-11097.
- 15 (a) H. Chen, Q. Zhao, Y. Wu, F. Li, H. Yang, T. Yi and C. Huang, *Inorg. Chem.*, 2007, 46, 11075-11081; (b) D.-L. Ma, W.-L. Wong, W.-H. Chung, F.-Y. Chan, P.-K. So, T.-S. Lai, Z.-Y. Zhou, Y.-C. Leung and K.-Y. Wong, *Angew. Chem. Int. Ed.*, 2008, 47, 3735-3739; (c) Q. Zhao, F. Li and C. Huang, *Chem. Soc. Rev.*, 2010, 39, 3007-3030; (d) Y. You, S. Cho and W. Nam, *Inorg. Chem.*, 2014, 53, 1804-1815; (e) M. Marín-Suárez, B. F. E. Curchod, I. Tavernelli, U. Rothlisberger, R. Scopelliti, I. Jung, D. Di Censo, M. Grätzel, J. F. Fernández-Sánchez, A. Fernández-Gutiérrez, M. K. Nazeeruddin and E. Baranoff, *Chem. Mater.*, 2012, 24, 2330-2338; (f) Y. You, Y. Han, Y.-M. Lee, S. Y. Park, W. Nam and S. J. Lippard, *J. Am. Chem. Soc.*, 2011, 133, 11488-11491.
- 16 (a) Q. Zhao, M. Yu, L. Shi, S. Liu, C. Li, M. Shi, Z. Zhou, C. Huang and F. Li, *Organometallics*, 2010, 29, 1085-1091; (b) X. Wang, J. Jia, Z. Huang, M. Zhou and H. Fei, *Chem. Eur. J.*, 2011, 17, 8028-8032; (c) Q. Zhao, C. Huang and F. Li, *Chem. Soc. Rev.*, 2011, 40, 2508-2524.
- 17 S. P.-Y. Li, C. T.-S. Lau, M.-W. Louie, Y.-W. Lam, S. H. Cheng and K. K.-W. Lo, *Biomaterials*, 2013, 34, 7519-7532.
- 18 (a) T. Murase, T. Yoshihara and S. Tobita, *Chem. Lett.*, 2012, 41, 262-263; (b) T. Yoshihara, A. Kobayashi, S. Oda, M. Hosaka, T. Takeuchi and S. Tobita, in *Proc. SPIE 8233, Reporters, Markers, Dyes*,

[Insert Running title of <72 characters]

- Nanoparticles, and Molecular Probes for Biomedical Applications IV*, San Francisco, CA, USA, 2012, pp. 82330A-82338.
- 19 (a) Y. Li, Y. Liu and M. Zhou, *Dalton Trans.*, 2012, 41, 3807-3816; (b) E. Baranoff, B. F. E. Curchod, J. Frey, R. Scopelliti, F. Kessler, I. Tavernelli, U. Rothlisberger, M. Grätzel and M. K. Nazeeruddin, *Inorg. Chem.*, 2011, 51, 215-224; (c) Y. Zhou, W. Li, Y. Liu and M. Zhou, *ChemPlusChem*, 2013, 78, 413-418.
- 20 (a) L. Xiong, Q. Zhao, H. Chen, Y. Wu, Z. Dong, Z. Zhou and F. Li, *Inorg. Chem.*, 2010, 49, 6402-6408; (b) P.-K. Lee, W. H.-T. Law, H.-W. Liu and K. K.-W. Lo, *Inorg. Chem.*, 2011, 50, 8570-8579; (c) Y. Chen, L. Qiao, L. Ji and H. Chao, *Biomaterials*, 2014, 35, 2-13.
- 21 (a) S. Lamansky, P. Djurovich, D. Murphy, F. Abdel-Razzaq, H.-E. Lee, C. Adachi, P. E. Burrows, S. R. Forrest and M. E. Thompson, *J. Am. Chem. Soc.*, 2001, 123, 4304-4312; (b) S. Lamansky, P. Djurovich, D. Murphy, F. Abdel-Razzaq, R. Kwong, I. Tsyba, M. Bortz, B. Mui, R. Bau and M. E. Thompson, *Inorg. Chem.*, 2001, 40, 1704-1711.
- 22 (a) S. Zhang, M. Hosaka, T. Yoshihara, K. Negishi, Y. Iida, S. Tobita and T. Takeuchi, *Cancer Res.*, 2010, 70, 4490-4498; (b) T. Yoshihara, Y. Karasawa, S. Zhang, M. Hosaka, T. Takeuchi, Y. Iida, K. Endo, T. Imamura and S. Tobita, in *Proc. SPIE 7190, Reporters, Markers, Dyes, Nanoparticles, and Molecular Probes for Biomedical Applications*, San Jose, CA, USA, 2009, pp. 71900X-71908.
- 23 J. R. Manning and H. M. Davies, *Org. Synth.*, 2007, 84, 334-346.
- 24 C. Dardonville, C. Fernandez-Fernandez, S.-L. Gibbons, G. J. Ryan, N. Jagerovic, A. M. Gabilondo, J. J. Meana and L. F. Callado, *Bioorgan. Med. Chem.*, 2006, 14, 6570-6580.
- 25 J. V. Caspar and T. J. Meyer, *J. Am. Chem. Soc.*, 1983, 105, 5583-5590.



Scheme 1 Synthesis of IrMitoOlivine and IrMitoNIR. i) MBBA,  $\text{CH}_2\text{Cl}_2/\text{CH}_3\text{OH}$  (50 vol.%), 80 °C, 2-4 h; ii) HDABoc; DCC/HOBt/DMF, r.t., 24 h; iii) TFA/ $\text{CH}_2\text{Cl}_2$  (20 vol.%), r.t., 2 h; iv) TPPC5H10COOH, DCC/HOBt/DMF, r.t., 24 h;  $\text{NH}_4\text{PF}_6$ .  
171x150mm (300 x 300 DPI)

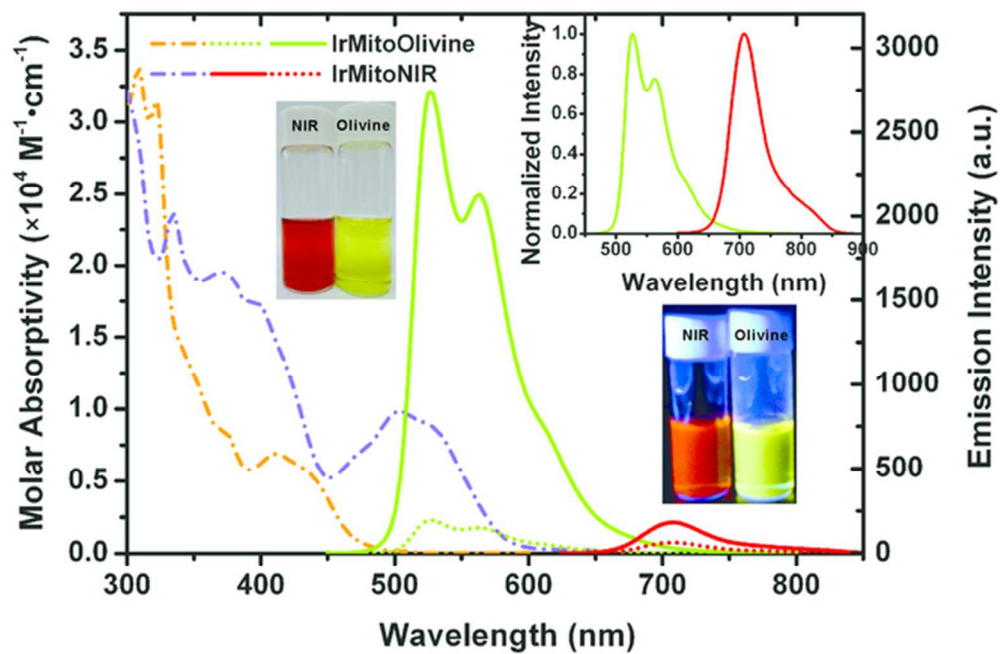


Fig. 1 Absorption (dash dot) and emission (solid: N<sub>2</sub>-saturated; dot: air-saturated) spectra of IrMitoOlivine and IrMitoNIR in CH<sub>3</sub>CN. The right top inset gives normalized emission spectra. Ex: IrMitoOlivine, 411 nm; IrMitoNIR, 504 nm. The photograph insets show the appearance of IrMitoOlivine and IrMitoNIR under natural (left top) and under UV (right bottom) light, respectively.  
56x37mm (300 x 300 DPI)

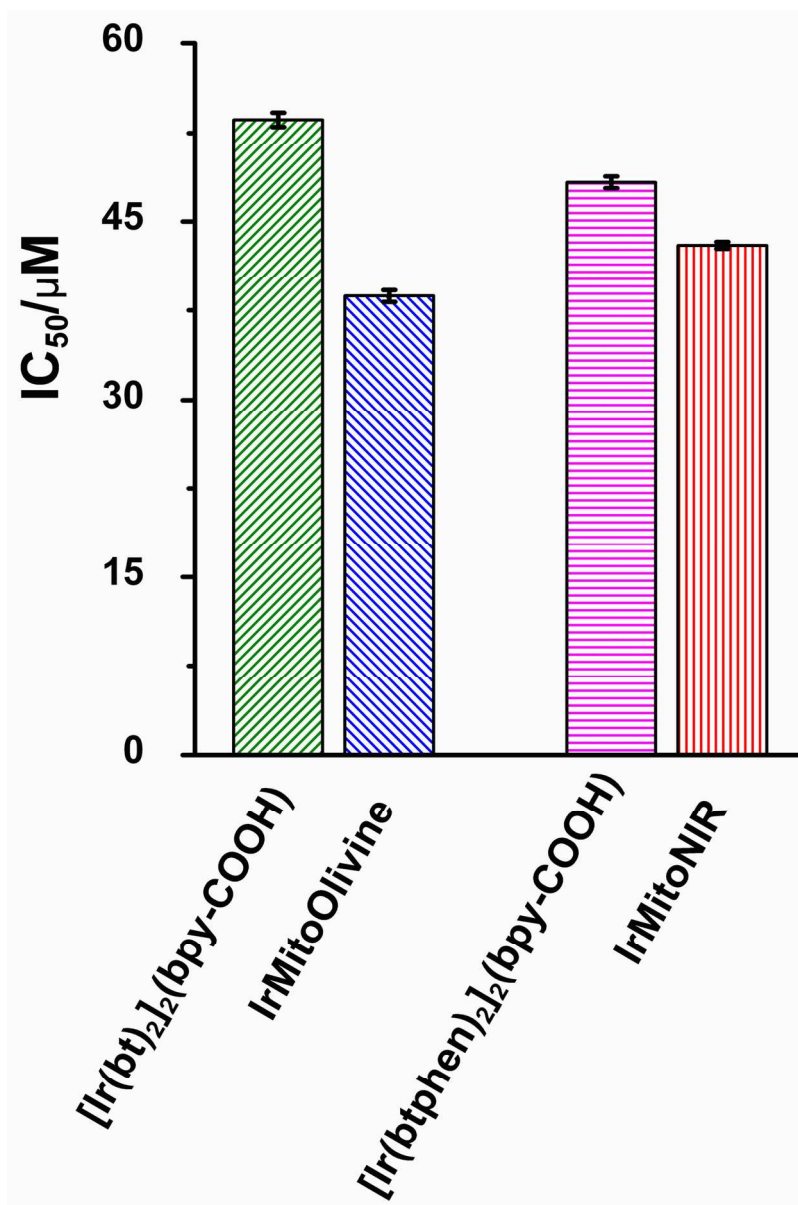


Fig. 2 Cytotoxicity (IC<sub>50</sub>) of IrMitoOlivine and IrMitoNIR in HeLa cells.  
127x190mm (300 x 300 DPI)

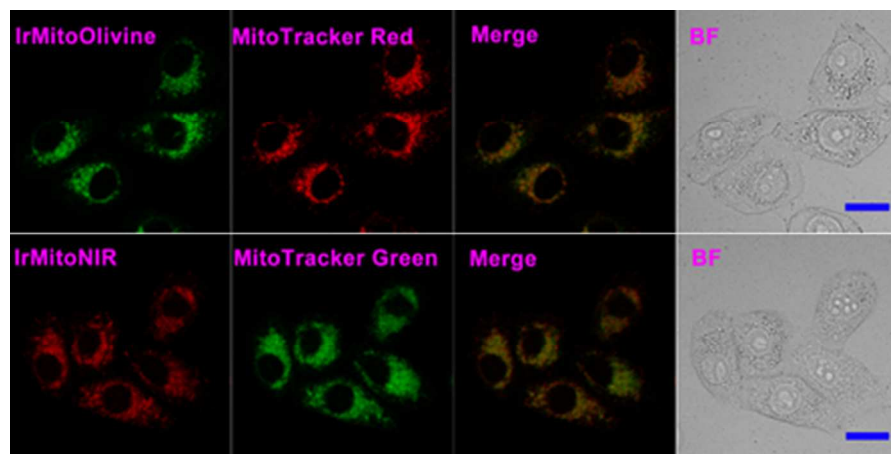


Fig. 3 Cell imaging of IrMitoOlivine and IrMitoNIR showed co-localization of MitoTracker® and IrMito dyes in HeLa Cells. Channel: FITC, Ex 488 nm, Em 500-530 nm; Cy5, Ex 561 nm, Em 662-737 nm. Scalar bar: 20 mm.  
37x18mm (300 x 300 DPI)

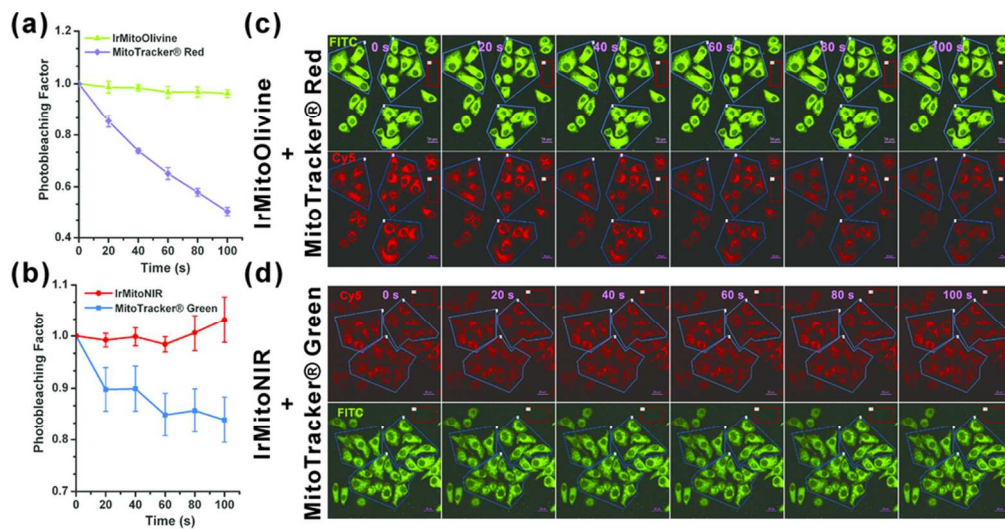
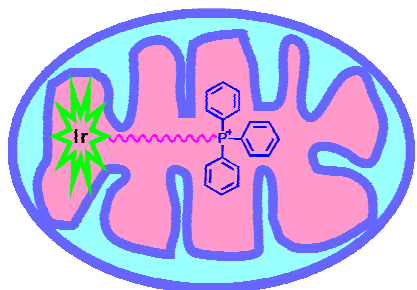


Fig. 4 Anti-photobleaching observation of IrMitoOlivine and IrMitoNIR in HeLa cells. (a) (b) Quantitative photobleaching results showed IrMitoOlivine and IrMitoNIR possessed robust emission intensity under continuous light irradiation. The data were represented as mean  $\pm$  standard deviation. (c) (d) Time-lapsed confocal imaging of IrMitoOlivine/MitoTracker® Red FM or IrMitoNIR/MitoTracker® Green FM co-stained HeLa cells. Blue and red ROIs represented three stochastically chosen cell-inclusive regions and the background region, respectively. Time interval: 20 s. Scalar bar: 20  $\mu$ m. 87x45mm (300 x 300 DPI)

## Graphical Abstract



Two phosphorescent iridium(III) complexes conjugated to lipophilic triphenylphosphonium cation showed high mitochondria-specificity and excellent anti-photobleachability under continuous laser irradiation.